Nickel K-Edge Extended X-Ray Absorption Fine Structure Studies of Bis(diamine) Nickel-(II) and -(III) Complexes*

John Evans, William Levason and Richard J. Perry
Department of Chemistry, University of Southampton, Southampton SO9 5NH, UK

Nickel and bromine K-edge extended X-ray absorption fine structure (EXAFS) data combined with UV/VIS spectroscopy have been used to study a range of $Ni(L-L)_2X_2$ complexes [X = Cl or Br; L–L = $H_2NCH_2CH_2NH_2$ (en), $H_2NCHMeCH_2NH_2$ (pn), $H_2N(CH_2)_3NH_2$ (tn), $MeHNCH_2CH_2NH_2$, $Me_2NCH_2CH_2NH_2$, $MeHNCH_2CH_2NHMe$ or $Me_2NCH_2CH_2NHMe$]. The data are consistent with pseudo-octahedral *cis*-N_4X_2 donor sets. In two cases only was there clear evidence in the EXAFS of back scattering from a second nickel centre indicative of a halide-bridged dimer formulation $[(L-L)_2Ni(\mu-X)_2Ni(L-L)_2]X_2$. The synthesis and properties of some nickel(III) complexes *trans*-$[Ni(L-L)_2X_2]X$ are described.

We[1] recently reported nickel K-edge extended X-ray absorption fine structure (EXAFS) studies on a variety of $[Ni(L-L)_3]^{2+/3+}$ (L–L = a diamine ligand) complexes. Here we report on similar studies on $Ni(L-L)_2X_2$ (X = Cl or Br) complexes, and some nickel(III) analogues. In some cases halogen oxidation of nickel(II) diamines leads to mixed-valence semiconductors, *e.g.* $[Ni^{II}(en)_2{\cdot}Ni^{IV}(en)_2Cl_2]_nCl_{4n}$ (en = $H_2NCH_2CH_2NH_2$), which have been previously studied by the EXAFS technique.[2,3] One aim of the present work was to obtain comparable data on nickel(II) and nickel(III) diamine complexes, which will be of value in further studies of the more complex mixed-valence systems. Although nickel(II) diamines have been the subject of extensive spectroscopic studies,[4] limited structural data are available, whilst the nickel(III) complexes are much less well established than examples with azamacrocycles[5] or heavier Group 15 donor ligands.[6,7]

Experimental

Physical measurements were made as described previously.[1] The nickel(II) diamine complexes were prepared by the same general method, one example of which is described. All had satisfactory analyses.

$[\{Ni(en)_2Cl\}_2]Cl_2$.—Nickel(II) chloride hexahydrate (3 g, 13 mmol) was dissolved in dry ethanol (20 cm^3) and 2,2-dimethoxypropane (5 cm^3) added. The mixture was refluxed under dry nitrogen until a yellow solution was obtained, cooled to room temperature, and ethylenediamine (1.7 cm^3, 25 mmol) in ethanol (5 cm^3) added. The blue solution was treated with diethyl ether with vigorous stirring until a blue solid separated. This was filtered off using standard Schlenk techniques and dried *in vacuo* (*ca.* 50%). The blue solid was stored in a sealed container in a dry-box until required.

Similar complexes were made with 1,2-diaminopropane (pn), 1,3-diaminopropane (tn), *N*-methylethylenediamine, *N,N*-dimethylethylenediamine, *N,N'*-dimethylethylenediamine and *N,N,N'*-trimethylethylenediamine. The complexes of some of the *N*-alkylated diamines are hygroscopic, and the water can replace the X groups in the first co-ordination sphere of the nickel for the *N,N*-dimethyl- and *N,N,N'*-trimethyl-ethylenediamine complexes. Complexes of the other *N*-alkylated diamine ligands change colour on prolonged exposure to moisture, but replacement of the X groups by water is incomplete.

Nickel(III) *Complexes*.—The complexes $[Ni(en)_2X_2]X$ and $[Ni(tn)_2X_2]X$ were made as previously reported.[8] The other complexes were made as described below.

The nickel(II) complex (2 mmol) was vacuum dried at 100 °C and after cooling was suspended in dry CCl_4 (25 cm^3) in a Schlenk flask. A solution of chlorine in dry CCl_4 was placed in second flask, and a slow stream of dry nitrogen passed *over* the solution, and the resulting vapour was bubbled into the suspension of the nickel diamine complex. After several hours the resulting solid was isolated using standard Schlenk techniques, and dried *in vacuo*. Yields *ca.* quantitative. The moisture-sensitive product was stored in a dry-box in a sealed container {Found for $[Ni(en)_2Cl_2]Cl$: C, 16.9; H, 5.8; N, 19.4. $C_4H_{16}Cl_3N_4Ni$ requires C, 16.8; H, 5.6; N, 19.6. Found for $[Ni(tn)_2Cl_2]Cl$: C, 23.1; H, 6.3; N, 17.7. $C_6H_{20}Cl_3N_4Ni$ requires C, 23.0; H, 6.4; N, 17.9. Found for $[Ni(MeHNCH_2CH_2NH_2)_2Cl_2]Cl$: C, 22.9; H, 6.6; N, 17.7. $C_6H_{20}Cl_3N_4Ni$ requires C, 23.0; H, 6.4; N, 17.9. Found for $[Ni(MeHNCH_2CH_2NHMe)_2Cl_2]Cl$: C, 28.4; H, 7.1; N, 16.3. $C_8H_{24}Cl_3N_4Ni$ requires C, 28.1; H, 7.0; N, 16.4. Found for $[Ni(en)_2Br_2]Br$: C, 11.6; H, 3.8; N, 13.7. $C_4H_{16}Br_3N_4Ni$ requires C, 11.5; H, 3.9; N, 13.4. Found for $[Ni(tn)_2Br_2]Br$: C, 16.3; H, 4.6; N, 12.3. $C_6H_{20}Br_3N_4Ni$ requires C, 16.1; H, 4.5; N, 12.5. Found for $[Ni(MeHNCH_2CH_2NH_2)_2Br_2]Br$: C, 16.0; H, 4.6; N, 12.3. $C_6H_{20}Br_3N_4Ni$ requires C, 16.1; H, 4.5; N, 12.5%}.

EXAFS data were collected in transmission mode on station 7.1 at the Daresbury Synchrotron Radiation Source, with an operating energy of 2 GeV (*ca.* 3.2 × 10^{-10} J) and currents of *ca.* 200 mA. A silicon(111) order-sorting monochromator was used, with harmonic rejection achieved by stepping off the rocking curve by 50% of full-height level. Samples were diluted with dry boron nitride, and run in aluminium spacers (1 mm thick) between Sellotape strips. Moisture-sensitive samples were made up in a dry-box, and stored in a desiccator until required. Infrared spectra of the complexes were routinely recorded to check for the absence of water. Data treatment was carried out using the programs PAXAS and EXCURVE 88 as described previously.[1] The nickel K-edge data sets were truncated at k = 12 $Å^{-1}$, and the bromine K-edge data at k = 10.5 $Å^{-1}$. The bromine data were Fourier filtered with a window of 1.5–5 Å, but for the nickel-edge data the raw EXAFS data were used.

---

* *Non-SI unit employed:* B.M. ≈ 0.927 × 10^{-23} A m^2.

Results and Discussion

Nickel(II) *Complexes*.—The nickel(II) diamine complexes $Ni(L–L)_2X_2$ (X = Cl or Br; L–L = en, pn, tn, $MeHNCH_2CH_2NH_2$, $Me_2NCH_2CH_2NH_2$, $MeHNCH_2CH_2NHMe$ or $Me_2NCH_2CH_2NHMe$) were made by combination of the appropriate nickel halide and the diamine under anhydrous conditions in alcohol, and the 2:1 stoichiometry confirmed by analytical data. Previous studies[4,9–13] have established that the nickel is six-co-ordinate, but the detailed structures are less clear, *trans* or *cis* monomers and *cis* halide-bridged dimers having been proposed for various complexes. The $Ni(en)_2Cl_2$ has been shown to have a $[(en)_2Ni(\mu\text{-}Cl)_2Ni(en)_2]Cl_2$ structure (Fig. 1) by single crystal X-ray methods,[9] but the other assignments are based upon IR or UV/VIS data, and the possibility that aqua complexes might have formed were not always considered. In the present work the anhydrous nature of the samples studied was confirmed by IR spectroscopy both before and after data collection. Diffuse reflectance UV/VIS spectra were recorded from powdered samples diluted with $BaSO_4$, in sealed silica cells, and the results are given in Table 1. For octahedral (O_h) Ni^{II}, three spin-allowed d–d bands are expected, in order of increasing energy ${}^3A_{2g} \longrightarrow {}^3T_{2g}$, ${}^3A_{2g} \longrightarrow {}^3T_{1g}$, ${}^3A_{2g} \longrightarrow {}^3T_{1g}(P)$. When the symmetry is lowered to D_{4h} (*trans*) or C_{2v} (*cis*, either mono- or di-nuclear) the degeneracies are lifted. In practice the *cis* isomers rarely show resolved band splittings, but for the *trans* isomers, the lowest energy band in particular is clearly split.[14] Comparison of the diffuse reflectance data of the diamine complexes in Table 1 with that of $[(en)_2Ni(\mu\text{-}Cl)_2Ni(en)_2]Cl_2$ which is known to be a (*cis*) chloro-bridged dimer, suggests that all have a similar donor symmetry (C_{2v}), although distinction between dimer and monomer structures is not possible on this basis. Table 1 also contains data on two complexes whose spectra are clearly different. These complexes decomposed on exposure to air and can be formulated as *trans*-$[Ni(L–L)_2(H_2O)_2]Br_2$ (L–L = $Me_2NCH_2CH_2NH_2$ or $Me_2NCH_2CH_2NHMe$).

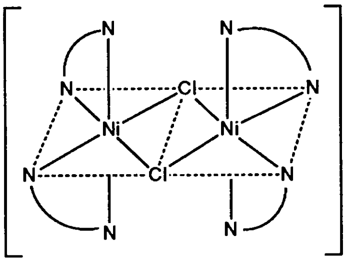

Fig. 1 The structure of $[(en)_2Ni(\mu\text{-}Cl)_2Ni(en)_2]Cl_2$

Table 1 Diffuse reflectance UV/VIS data for the $Ni(L–L)_2X_2$ complexes *

Complex	ν_1/cm^{-1}	ν_2/cm^{-1}	ν_3/cm^{-1}
$Ni(en)_2Cl_2$	10 530	17 000	26 700
$Ni(en)_2Br_2$	10 420	17 100	27 000
$Ni(pn)_2Cl_2$	10 550	17 000	26 500
$Ni(pn)_2Br_2$	10 500	17 100	26 700
$Ni(tn)_2Cl_2$	8 025	17 420	28 900
$Ni(tn)_2Br_2$	7 910	17 120	27 175
$Ni(MeHNCH_2CH_2NH_2)_2Cl_2$	8 330	17 760	26 450
$Ni(MeHNCH_2CH_2NH_2)_2Br_2$	7 355	17 480	26 880
$Ni(Me_2NCH_2CH_2NH_2)_2Cl_2$	9 850	15 900	25 800
$Ni(Me_2NCH_2CH_2NH_2)_2Br_2$	9 090	15 600	25 000
$Ni(MeHNCH_2CH_2NHMe)_2Cl_2$	8 330	16 700	26 200
$Ni(MeHNCH_2CH_2NHMe)_2Br_2$	7 575	16 700	26 100
$Ni(Me_2NCH_2CH_2NHMe)_2Cl_2$	8 265	15 100	24 700
$Ni(Me_2NCH_2CH_2NHMe)_2Br_2$	7 400	16 800	26 200
$[Ni(Me_2NCH_2CH_2NH_2)_2(H_2O)_2]Br_2$	8 930 11 630 (sh)	16 900	26 700
$[Ni(Me_2NCH_2CH_2NHMe)_2(H_2O)_2]Br_2$	8 900 11 100 (sh)	16 500	26 200

* Samples diluted with $BaSO_4$. Frequencies ν_1, ν_2, ν_3 are related to the ${}^3A_{2g} \longrightarrow {}^3T_{2g}$, ${}^3A_{2g} \longrightarrow {}^3T_{1g}$ and ${}^3A_{2g} \longrightarrow {}^3T_{1g}(P)$ transitions in O_h symmetry: despite the lower symmetry (C_{2v}) band splittings are not resolved for the halogeno complexes although the peak shapes are asymmetric.

Nickel(III) *Complexes*.—Halogen oxidation of the $Ni(L–L)_2X_2$ complexes is known to give mixed-valence Ni^{II}–Ni^{IV}

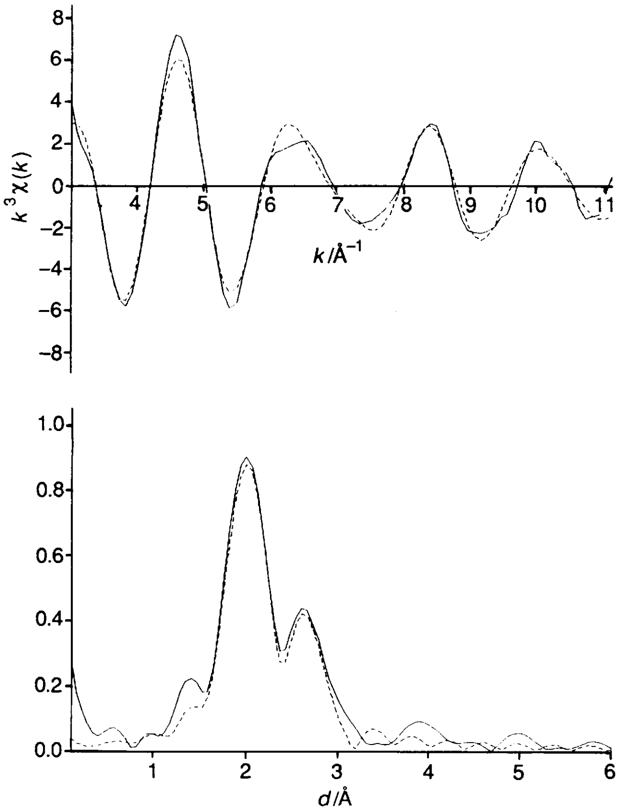

Fig. 2 The background-subtracted nickel K-edge EXAFS (——, experimental × k^3; – – –, curved-wave theory × k^3) and Fourier transform (——, experimental; – – –, theoretical) for $[(en)_2Ni(\mu\text{-}Br)_2Ni(en)_2]Br_2$

Table 2 Spectroscopic data for the $[Ni(L–L)_2X_2]X$ complexes

Complex	Colour	μ/B.M.	$E_{max}{}^a/cm^{-1}$	$g_\perp{}^b$	$g_\parallel{}^b$
$[Ni(en)_2Cl_2]Cl$	Orange	1.91	13 150 (br), 20 700 (sh), 23 800 (sh), 27 250	2.19	2.03
$[Ni(tn)_2Cl_2]Cl$	Orange	1.95	12 700 (br), 22 990 (sh), 25 970 (sh), 28 400	2.17	2.04
$[Ni(MeHNCH_2CH_2NH_2)_2Cl_2]Cl$	Mustard	1.96	13 500 (br), 20 000 (sh), 27 170 (sh), 34 250	2.19	2.05
$[Ni(MeHNCH_2CH_2NHMe)_2Cl_2]Cl$	Brown	1.91	13 150 (br), 20 400 (sh), 23 250 (sh), 26 880	2.04	2.20
$[Ni(en)_2Br_2]Br$	Brown	1.82	11 860 (br), 17 800 (sh), 24 700 (sh), 26 300	2.13	
$[Ni(tn)_2Br_2]Br$	Brown	1.99	11 850 (sh), 17 350 (sh), 22 600 (sh), 25 380	2.14	
$[Ni(MeHNCH_2CH_2NH_2)_2Br_2]Br$	Red-brown	1.90	12 000 (sh), 17 100 (sh), 24 400 (sh), 29 400		

[a] Diffuse reflectance data, samples diluted with $BaSO_4$. [b] Room temperature ESR data for powdered solids, referenced to diphenylpicrylhydrazyl.

materials for L–L = pn or en, and nickel(III) complexes $[Ni(L\text{–}L)_2X_2]X$ for L–L = en or tn.[8,15] The en and tn complexes were reprepared in this work and the data on them (Table 2) is in good agreement with the literature data. Although a nickel(III) complex of pn has been claimed,[16] in our hands only the known[8,15] Ni^{II}–Ni^{IV} mixed-valence material was obtained. Oxidation of $Ni(L\text{–}L)_2X_2$ suspended in CCl_4 with the corresponding halogen heavily diluted with nitrogen, gave moisture-sensitive $[Ni(L\text{–}L)_2X_2]X$ complexes for L–L = $MeHNCH_2CH_2NH_2$, X = Cl or Br and L–L = $MeHNCH_2CH_2NHMe$, X = Cl, but for both complexes of $Me_2NCH_2CH_2NHMe$ and $Me_2NCH_2CH_2NH_2$, and the $MeHNCH_2CH_2NHMe$, X = Br combination, decomposition occurred. The isolated complexes are formulated as nickel(II) complexes on the basis of their spectroscopic properties (Table 2). The magnetic moments are consistent with a low-spin d^7 Ni^{III}, and the ESR spectra confirm the unpaired electron is metal centred. Three of the chlorides have $g_{\perp} > g_{\parallel}$ consistent with a tetragonally elongated environment, but curiously for $[Ni(MeHNCH_2CH_2NHMe)_2Cl_2]Cl$ the ESR g values are reversed suggesting an axially compressed geometry. The $[Ni(MeHNCH_2CH_2NH_2)_2Br_2]Br$ complex failed to exhibit an ESR spectrum despite its paramagnetism, an effect occasionally observed with other nickel(III) complexes including [Ni-

Table 3 Nickel K-edge EXAFS data on the nickel(II) and nickel(III) complexes[a]

Complex	Shell	d/Å	$2\sigma^{2\,b}$/Å^2	R^c (%)
$Ni(en)_2Cl_2$	4N	2.085(7)	0.012(06)	28.0
	2Cl	2.467(5)	0.021(1)	
	4C	2.899(10)	0.019(2)	
$Ni(en)_2Br_2$	4N	2.059(3)	0.010(4)	14.2
	2Br	2.578(9)	0.029(2)	
	4C	2.287(10)	0.010(2)	
	1Ni	3.892(13)	0.020(3)	
$Ni(pn)_2Cl_2$	4N	2.064(3)	0.014(06)	21.4
	2Cl	2.431(5)	0.021(09)	
	4C	2.865(7)	0.014(2)	
$Ni(pn)_2Br_2$	4N	2.071(2)	0.009(03)	18.6
	2Br	2.616(2)	0.022(08)	
	4C	2.889(5)	0.009(1)	
	1Ni	3.893(10)	0.022(2)	
$Ni(tn)_2Cl_2$	4N	2.067(3)	0.016(04)	17.2
	2Cl	2.433(4)	0.018(1)	
	4C	2.751(15)	0.031(6)	
	2C	3.030(20)	0.016(4)	
$Ni(tn)_2Br_2$	4N	2.064(2)	0.010(03)	20.1
	2Br	2.591(3)	0.022(06)	
	4C	2.917(15)	0.036(6)	
	2C	3.106(11)	0.009(2)	
$Ni(MeHNCH_2CH_2NH_2)_2Cl_2$	4N	2.071(4)	0.010(05)	24.7
	2Cl	2.449(7)	0.021(1)	
	6C	2.841(10)	0.025(2)	
$Ni(MeHNCH_2CH_2NH_2)_2Br_2$	4N	2.077(3)	0.010(04)	22.7
	2Br	2.625(7)	0.029(2)	
	6C	2.867(10)	0.026(3)	
$Ni(Me_2NCH_2CH_2NH_2)_2Cl_2$	4N	2.058(5)	0.014(1)	19.9
	2Cl	2.432(6)	0.019(1)	
	8C	2.869(9)	0.030(2)	
$Ni(Me_2NCH_2CH_2NH_2)_2Br_2$	4N	2.097(4)	0.017(07)	25.2
	2Br	2.557(4)	0.022(07)	
	8C	2.909(7)	0.025(2)	
$Ni(MeHNCH_2CH_2NHMe)_2Cl_2$	4N	2.073(4)	0.012(06)	24.7
	2Cl	2.407(8)	0.025(1)	
	8C	2.814(10)	0.034(3)	
$Ni(MeHNCH_2CH_2NHMe)_2Br_2$	4N	2.087(4)	0.011(06)	21.9
	2Br	2.610(9)	0.028(2)	
	8C	2.871(18)	0.047(5)	
$Ni(Me_2NCH_2CH_2NHMe)_2Cl_2$	4N	2.096(4)	0.014(07)	22.5
	2Cl	2.376(4)	0.011(05)	
	10C	2.853(12)	0.044(3)	
$Ni(Me_2NCH_2CH_2NHMe)_2Br_2$	4N	2.095(3)	0.013(06)	26.4
	2Br	2.543(4)	0.021(07)	
	10C	2.873(8)	0.034(2)	
$[Ni(en)_2Cl_2]Cl$	4N	1.917(1)	0.008(02)	13.2
	2Cl	2.423(2)	0.015(04)	
	4C	2.753(4)	0.012(08)	
$[Ni(en)_2Br_2]Br$	4N	1.915(1)	0.011(02)	13.8
	2Br	2.582(2)	0.020(04)	
	4C	2.718(9)	0.024(2)	
$[Ni(tn)_2Cl_2]Cl$	4N	1.972(1)	0.012(02)	16.5
	2Cl	2.386(2)	0.020(04)	
	4C	2.911(10)	0.041(3)	
	2C	3.385(8)	0.014(2)	

[a] Standard deviations in parentheses. Note that the systematic errors in bond distances arising from the data collection and analysis procedures are *ca.* 0.02–0.03 Å for well defined co-ordination shells. [b] Debye–Waller factor. [c] R factor defined as $[\int(\chi^T - \chi^E)k^3dk/\int\chi^E k^3dk] \times 100$.

Table 4 Bromine K-edge EXAFS data on nickel(II) complexes*

Complex	Shell	d/Å	$2\sigma^2$/Å^2	R (%)
$Ni(en)_2Br_2$	1Ni	2.606(3)	0.026(05)	26.6
	3N	3.370(7)	0.028(2)	
	0.5Br	3.517(5)	0.016(1)	
$Ni(pn)_2Br_2$	1Ni	2.606(2)	0.025(04)	20.4
	3N	3.364(6)	0.028(1)	
	0.5Br	3.520(5)	0.018(1)	
$Ni(MeHNCH_2CH_2NH_2)_2Br_2$	1Ni	2.605(3)	0.0286(05)	28.6
	3N	3.311(6)	0.0167(1)	
	0.5Br	3.458(6)	0.0178(2)	
$Ni(MeHNCH_2CH_2NHMe)_2Br_2$	1Ni	2.599(2)	0.023(04)	23.5
	3N	3.324(6)	0.028(2)	
	0.5Br	3.455(5)	0.016(1)	
$Ni(Me_2NCH_2CH_2NH_2)_2Br_2$	1Ni	2.546(2)	0.024(03)	21.0
	3N	3.306(6)	0.030(1)	
	0.5Br	3.446(9)	0.028(2)	

* See footnotes to Table 3. The bromine-edge data were Fourier filtered with a window 1.5–5 Å to remove low R features.

$(PMe_2Ph)_2Br_3]$[17] and presumably due to unfavourable relaxation effects. The electronic spectra all contain a weak feature at *ca.* 12 000 cm^{-1} which can be assigned to the $^2A_{2g} \longrightarrow {}^2B_{1g}$ transition in D_{4h} symmetry,[18] with the higher energy features > *ca.* 20 000 cm^{-1} mostly assignable as $\pi(X) \longrightarrow$ Ni and $\sigma(N) \longrightarrow$ Ni charge transfer.

EXAFS Studies.—Nickel K-edge data. The general approach followed that described for the $[Ni(L{-}L)_3]X_2$ complexes,[1] with shells being added stepwise, iterated and the fits tested for statistical significance. The data treatment for these complexes was developed using $Ni(en)_2Cl_2$ as a model (Fig. 1), since single crystal X-ray data are available[9,19] which confirm the structure as $[(en)_2Ni(\mu\text{-}Cl)_2Ni(en)_2]Cl_2$. The X-ray data revealed that the chloride bridges are asymmetric with d(Ni–Cl) 2.471(1) and 2.561(1) Å, and d(Ni–N) ranging from 2.087(1) to 2.117(1) Å (average = 2.097 Å). The full theoretical model would thus be 4N:1Cl:1Cl:4C:1Ni. Fitting this model to the raw data gave satisfactory agreement in the d(Ni–N), but the attempt to split the chlorine shells failed, the separate shells failing the statistical test[20] and with the distances highly correlated. The chlorine shells were amalgamated which resulted in a marked improvement, although the Debye–Waller factor was larger than usual, probably reflecting the static disorder in the chlorine shell. There was no significant feature in the Fourier transform at *ca.* 3.7 Å where the nickel shell was expected, and attempts to add such a shell failed the statistical tests.[20,21] The final best fit is shown in Table 3. The treatment of the data from the other $Ni(L{-}L)_2Cl_2$ complexes followed similarly, the modelling of the diamine ligands being the same as developed[1] for the $[Ni(L{-}L)_3]X_2$ complexes, essentially that for *N*-methylated ligands, a single carbon shell for N–Me and N–C(backbone) was used, for tn two carbon shells N–C and NC–C, but for pn the NC–Me group was not included since addition of such a shell failed the statistical tests. The final fits are summarised in Table 3 and representative examples are in Fig. 2. The bond lengths seem internally consistent within the normal precision of EXAFS data (±0.02–0.03 Å) and are also in keeping with the limited X-ray crystallographic data.[9,19,22–24]

The $Ni(en)_2Br_2$ complex is known to be isostructural with the chloride,[25,26] and the nickel data treatment used similar models to the chlorides, again with a single shell for the halide ligands. However, in two cases, $Ni(en)_2Br_2$ and $Ni(pn)_2Br_2$, there was evidence for a further feature in the Fourier transforms at *ca.* 3.9 Å, and in each case when a nickel shell was added to the model it passed the Joyner test.[21] We conclude that the d(Ni $\cdots$ Ni) is evident in the EXAFS data, but is a small component of the back scattering and correspondingly not well defined. Attempts to add a shell corresponding to the remote nickel were unsuccessful in the cases of the other bromide complexes.

In summary, the nickel K-edge EXAFS data on both series of complexes were fitted well by a model based upon an N_4X_2 donor set, but in the majority of cases did not in isolation discriminate between *trans*-, *cis*-monomer or *cis* dimer structures. For two of the bromides, identification of a weak feature ascribed the remote nickel shell supported by the *cis* dimer geometry.

Bromine K-edge data. Further information can be obtained *via* the halogen K-edge EXAFS data. Unfortunately at the time of this study technical problems with the SOXAFS station resulted in chlorine-edge data of very poor quality, and these provided no useful information. However, data at the harder bromine K-edge were obtained for most of the complexes and analysed using three models, 1Ni:3N:0.5Br, 1Ni:3N:1Br and 1Ni:4N, corresponding to *cis*-dimer, *cis*-monomer and *trans* geometries respectively.* The *trans* model gave a very poor fit and was rejected, but the *cis*-dimer model gave results in good agreement with the nickel-edge data (Table 4). Changing the occupation number of shell 3 from 0.5 to 1, corresponding to the *cis*-monomer model, caused only small changes in the R factor, but gave a large increase in the Debye–Waller factor for the shell. Whilst this may suggest that the *cis* dimer is the more realistic model, the assignment of structure on this basis alone is uncertain due to the correlation between the occupation number and Debye–Waller factor.

Nickel(III) *complexes.* The nickel(III) diamine complexes of the *N*-methylated ligands decomposed on standing even in sealed containers, and only the en and tn complexes were studied (Table 3). The nickel-edge EXAFS data for the two en complexes were modelled to a N_4X_2 model and refined to give d(Ni–N) of 1.91 Å, substantially shorter than the value of *ca.* 2.1 Å observed in the nickel(II) dimers. Comparison of the d(Ni–X) distances with those of other *trans*-$[Ni(L{-}L)_2X_2]^+$ shows good agreement, *e.g.* $[Ni\{o\text{-}C_6H_4(AsMe_2)_2\}_2Cl_2]^+$ 2.42 Å[27] and $[Ni\{o\text{-}C_6F_4(AsMe_2)_2\}_2Br_2]^+$ 2.54 Å.[28]

Conclusion

The combination of the UV/VIS spectroscopic data and nickel and bromine K-edge EXAFS data demonstrates that the $Ni(L{-}L)_2X_2$ complexes contain *cis*-N_4X_2 donor sets and provides bond length information about the nickel centre. Direct evidence for the second nickel centre was found in only two of the bromide complexes indicating that they should be formulated as $[(L{-}L)_2Ni(\mu\text{-}Br)_2Ni(L{-}L)_2]Br_2$ (L–L = en or pn). Even

---

* There are also unco-ordinated bromide ions in the lattice which contribute to the EXAFS, but which were not fitted. This accounts in part for the high R factors.

for the $Ni(en)_2Cl_2$ complex which is known from single crystal X-ray studies to be a dimer, this was not evident in the EXAFS data. From the similarity of the spectroscopic properties it seems likely that most (or all) of the complexes studied are dimers, but the EXAFS data fail to provide supporting evidence in the majority of cases. The observation of back scattering from neighbouring nickel centres in the linear chain materials is similarly difficult.[2,3]

Acknowledgements

We thank the Director of the Daresbury Laboratory for the provision of facilities and the SERC for support (to R. J. P.).

References

1 J. Evans, W. Levason and R. J. Perry, *J. Chem. Soc., Dalton Trans.*, 1990, 3691.

2 J. Evans, J. T. Gauntlett and W. Levason, *Inorg. Chem.*, 1988, **27**, 4521.

3 K. Toriumi, T. Kanao, Y. Umetsu, A. Ohyoshi, M. Yamashita and T. Ito, *J. Coord. Chem.*, 1988, **19**, 181.

4 L. Sacconi, F. Mani and A. Bencini, in *Comprehensive Coordination Chemistry*, eds. G. Wilkinson, J. A. McCleverty and R. D. Gillard, Pergamon, Oxford, 1987, vol. 5, p. 1.

5 A. G. Lappin and A. McAuley, *Adv. Inorg. Chem.*, 1988, **32**, 241.

6 L. R. Gray, S. J. Higgins, W. Levason and M. Webster, *J. Chem. Soc., Dalton Trans.*, 1984, 459.

7 J. M. Corker, J. Evans, W. Levason, M. D. Spicer and P. Andrews, *Inorg. Chem.*, 1991, **30**, 331.

8 D. A. Cooper, S. J. Higgins and W. Levason, *J. Chem. Soc., Dalton Trans.*, 1983, 2131.

9 K. O. Joung, C. J. O'Connor, E. Sinn and R. L. Carlin, *Inorg. Chem.*, 1979, **18**, 804.

10 D. M. L. Goodgame and L. M. Venanzi, *J. Chem. Soc.*, 1963, 616, 5909.

11 I. Bertini and L. Mani, *Inorg. Chim. Acta*, 1969, **3**, 451.

12 C. W. Schlapfer, Y. Saito and K. Nakamoto, *Inorg. Chim. Acta*, 1972, **6**, 284.

13 A. B. P. Lever and E. Mantovani, *Can. J. Chem.*, 1973, **51**, 1567.

14 A. B. P. Lever, *Inorganic Electronic Spectroscopy*, Elsevier, Amsterdam, 2nd edn., 1984 and refs. therein.

15 M. Yamashita, Y. Nonaka, S. Kida, Y. Hamaue and R. Aoki, *Inorg. Chim. Acta*, 1981, **52**, 43.

16 A. K. Das and D. V. R. Rao, *J. Indian Chem. Soc.*, 1983, **60**, 718.

17 D. W. Meek, E. C. Alyea, J. K. Stalick and J. A. Ibers, *J. Am. Chem. Soc.*, 1969, **91**, 344.

18 G. V. R. Chandramouli and P. T. Manoharan, *Inorg. Chem.*, 1987, **26**, 3291.

19 G. A. Bottomley, L. G. Glossop, C. L. Raston, A. H. White and A. C. Willis, *Aust. J. Chem.*, 1978, **31**, 285.

20 N. Binsted, S. L. Cook, J. Evans, G. N. Greaves and R. J. Price, *J. Am. Chem. Soc.*, 1987, **109**, 3669.

21 R. W. Joyner, K. J. Martin and P. Meehan, *J. Phys. C*, 1987, **20**, 4005.

22 A. J. Finney, M. A. Hitchman, C. L. Raston, G. L. Rowbotton and A. H. White, *Aust. J. Chem.*, 1981, **34**, 2085.

23 A. J. Finney, M. A. Hitchman, C. L. Raston, G. L. Rowbottom and A. H. White, *Aust. J. Chem.*, 1981, **34**, 2047.

24 S. Garcia-Granda and F. Gomez-Beltran, *Acta Crystallogr., Sect. C*, 1984, **40**, 1145.

25 A. S. Antsyshkina and M. A. Porai-Koshits, *Dokl. Akad. Nauk SSSR*, 1962, **143**, 105.

26 A. P. Ginsberg, R. L. Martin, R. W. Brookes and R. C. Sherwood, *Inorg. Chem.*, 1972, **11**, 2884.

27 P. K. Bernstein, G. A. Rodley, R. Marsh and H. B. Gray, *Inorg. Chem.*, 1972, **11**, 3040.

28 L. R. Hanton, J. Evans, W. Levason, R. J. Perry and M. Webster, *J. Chem. Soc., Dalton Trans.*, 1991, 2039.

Received 19*th November* 1991; *Paper* 1/05877K